ELSEVIER

Ceramics International 32 (2006) 767–773

CERAMICS INTERNATIONAL

www.elsevier.com/locate/ceramint

STEM-X-EDS analysis of morphotropic PZT ceramics Analysis of Zr/Ti + Zr values fluctuation depending on microstructure and synthesis route of powders

Christian Courtois [a,*], Jacques Crampon [b], Philippe Champagne [a], Cedric Cochrane [c], Nathalie Texier [a], Anne Leriche [a]

[a] *Laboratoire Matériaux et Procédés, Université de Valenciennes et du Hainaut-Cambrésis, Zone Ind. du Champ de l'abbesse 59600 Maubeuge, France*

[b] *Laboratoire de Structure et Propriétés de l'Etat Solide, UMR-CNRS 8008, Bâtiment C 6, Université des Sciences et Technologies de Lille 59655 Villeneuve D'ascq Cedex, France*

[c] *ENSAIT 9, rue de l'Ermitage, BP 30329, 59056 Roubaix Cedex 01, France*

Received 14 March 2005; received in revised form 30 April 2005; accepted 19 May 2005
Available online 12 September 2005

Abstract

A TEM-EDS analysis technique is applied to estimate dopant incorporation and Zr/Zr + Ti fluctuation in morphotropic PZT ceramics starting from powders synthesized by two routes. A solid-state synthesis route leads to less reactive powders requiring severe conditions to reach full densification. The hydrothermal route leads to more reactive powders that can be fully densified at lower temperature. In addition, the influence of Ni addition was analyzed.

Zr/Zr + Ti fluctuations were estimated by the standard deviation of concentrations carried out by chemical analyses.

It was shown that there is no significant partitioning of Zr and Ti inside a grain or in the ceramic. Each PZT material appears to be homogenous with a constant value of standard deviation of Zr/Zr + Ti ratios. The obtained values depend mainly on the presence or not of Ni addition whatever the nature of the chosen synthesis route. Standard deviation values of Zr/Zr + Ti ratios appear to be in accordance with literature values estimated by high temperature X-ray diffraction broadening. Results are also discussed relatively to some piezoelectric properties and more particularly to the quality mechanical factor.

Keywords: A. Powders: chemical preparation; B. Electron microscopy; B. X-ray methods; D. PZT

1. Introduction

Lead zirconate titanate with general formula $Pb(Zr_xTi_{1-x})O_3$ (PZT) exhibits a complete solid solution between lead titanate $PbTiO_3$ (PT) and lead zirconate $PbZrO_3$ (PZ) [1] at room temperature. The ferroelectric region of the phase diagram consists mainly of two different regions: a Zr-rich rhombohedral region and a Ti-rich region; they are separated by a phase boundary which is nearly independent of the temperature. It is now well established that the tetragonal phase in the titanium-rich side of the binary system and the rhombohedral one in the zirconium-rich side are separate by a monoclinic phase around $x = 0.48$ [2]. The stable monoclinic phase recently discovered in the PZT system close to the morphotropic phase boundary (MPB) acts as a link between the rhombohedral and the tetragonal phase explaining the high piezoelectric activities usually observed around this MPB composition.

Many authors have tried to understand the nature of the MPB and of the phase stabilized around this specific composition. Several experimental difficulties explain why this transition is not clearly understood or why it is so difficult to compare results from one author to another.

* Corresponding author. Tel.: +33 3 2753 1669; fax: +33 3 2753 1667.
E-mail address: christian.courtois@univ-valenciennes.fr (C. Courtois).

0272-8842/$30.00 © 2005 Published by Elsevier Ltd and Techna Group S.r.l.
doi:10.1016/j.ceramint.2005.05.019

In PZT ceramics, experimental data concerning evidence of this MPB are based on the observation of specific X-ray diffraction pattern measured generally at ambient temperature.

The X-ray diffraction patterns are not easy to analyze. The occurrence of MPB is made obvious through the coexistence of a mixture of specific diffraction peaks (generally T + R, and for some M). But the exact positions of these peaks depend on strains, composition of each phase, whereas the shape and the broadening depends on microstrains, crystallite size and more specifically for this solid solution on chemical fluctuations Δx leading on d-spacing fluctuation and so multiple and additional broadening effects Δx in each phase. These multiple contributions affect the diffraction diagram in a complex way explaining why some discrepancies can be observed in the literature. They concern the position (in composition) of the MPB, the nature of the stabilized phases (in nature and in composition) and their homogeneities (in chemical composition (Zr/Ti + Zr) and microstrains ditributions).

Concerning chemical fluctuations, it can be admitted that some remain in the ceramic form as they are frozen in during the elaboration of the ceramic. These remained chemical fluctuations (in term of Zr and Ti location) perturb the ambient diffraction diagram. Some distributions of d-spacing, caused by these fluctuations, incite to a broadening of diffraction peaks. Cross and other authors [3,4] have proposed a model of PZT ceramics describing them as an aggregation of monophasic grains. It is assumed that the grain boundary motion, during the thermal treatment corresponding to the sintering step, flattened the chemical fluctuations in each grain. As a consequence, the chemical fluctuation amplitude is related to coarsening during sintering. Some dependence between grain growth and chemical fluctuation amplitude has been pointed out and experimentally verified. These results are based on the interpretation of the ambient X-ray diffraction pattern of prepared ceramics. The MPB is described as a mixture of rhombohedral and tetragonal phases; each phase having a specific composition. By means of XRD refinement, the composition of each phase and their amount are calculated. It is shown that the gap of composition of R and T phases (interpreted in terms of MPB width) decreases as the grain size increase. The dependence follows the relation $\Delta x \approx G^{-3}$. From an experimental point of view, the inverse dependency of the apparent composition gap, and therefore of the MPB width, on the quality of synthesis of PZT (powder synthesis routes, amplitude of pre-thermal treatment in oxide powder synthesis routes, sintering conditions ...) has been clearly shown. But their interpretation in terms of chemical fluctuations and apparent MPB width is linked to a hypothesis postulated for the interpretation of X-ray diffraction pattern and to the quality of refinement. More accurate experimental and interpreted results are probably those from Noheda et al. [2]. The X-ray diffraction pattern is registered at temperatures higher than the Curie transition temperature. The X-ray diffraction pattern consists of isolated cubic peaks. Their width (broadening) is explained in terms of d-spacing fluctuations resulting from chemical fluctuations. In addition, this analysis demonstrates the existence of a monoclinic phase. In that case, internal chemical fluctuations, for the pure PZT ceramics are very low $\Delta x \approx 0.003$ in the MPB range.

All these interpretations are dependent on the quality of X-ray diffraction registration and their refinement. Therefore, it would be interesting to have another way to measure those internal chemical fluctuations.

This is precisely the objective of this paper. We propose to estimate the amplitude of the chemical fluctuations directly by X-ray EDS analysis during TEM measurements.

We dispose of several doped PZT ceramics obtained starting from different powder sources. A first one consists of a solid-state synthesis route leading to not very reactive powders. In order to reach an almost full densification, the sintering conditions are quite severe. A second one consists of a chemical/hydrothermal synthesis route, leading to a more reactive powder. The sintering conditions are drastically lowered and permit the synthesis of dense ceramics. All these ceramics are multidoped in the same manner and exhibit at room temperature a complex X-ray diffraction pattern, characteristic for MPB.

These ceramics were very closely analyzed in terms of global chemical composition by means of X-ray fluorescence for $x = (Zr/Ti + Zr)$ ratio and ICP-AES for doping elements. On the other hand, some piezoelectric characteristics have been determined and could be useful for ultimate interpretation.

For this work, additional chemical analyses were done locally with a TEM-EDS equipment in the STEM mode using beam diameters of about 5 nm and allowing to compare (Zr/Ti + Zr) ratios and doping element concentrations, from one grain to another, by crossing throughout a grain and from one ferroelectric domain to another. The results are compared with the literature data.

2. Experimental

2.1. PZT ceramics

Two powders synthesis routes, described in detail in [5], have been used, a solid-state synthesis one (ceramics labeled C) and a hydrothermal one (ceramics labeled H). Their stoechiometric composition corresponds to the formula: $Pb(Zr_{0.49}Ti_{0.51})_{O.94}(Mn_{0.0252}Sb_{0.0192}W_{0.0156})O_3$. Four ceramics were analyzed: with and without 0.8758 mol% of nickel addition for both oxide and hydrothermal routes.

The nominal and global compositions of these ceramics have been determined and are presented in Table 1.

The main steps of solid-state synthesis route are as follows: (i) mixing of oxide powders, de-agglomeration in alcohol suspension; (ii) calcination at 820 °C, 5 h; (iii) final

Table 1
Composition of the different powders used in this work as starting materials for the realization of ceramics

	Composition (at.%)[a]				x[b]
	Mn	Sb	W	Ni	
Target values	0.504	0.384	0.312	0.175	0.49
Powders					
C	0.504 ± 4.10^{-3}	0.372 ± 0.012	0.340 ± 2.10^{-3}	–	0.50
C–Ni	0.510 ± 0.01	0.378 ± 0.01	0.342 ± 4.10^{-3}	0.185 ± 6.10^{-3}	0.49
H	0.544 ± 4.10^{-3}	0.386 ± 4.10^{-3}	0.344 ± 4.10^{-3}	–	0.50
H–Ni	0.534 ± 4.10^{-3}	0.400 ± 0.01	0.328 ± 4.10^{-3}	0.192 ± 0.01	0.48

[a] Determined by means of ICP-AES All numbers are significant.
[b] $x = ([Zr])/([Zr] + [Ti])$, [Zr] and [Ti] are determined by X-ray florescence. All numbers are significant.

de-agglomeration. Hydrothermal synthesis was conducted as follows: (i) mixing in alcohol of $Ti(^{i}PrO)_4$ and $Zr(^{n}PrO)_4$ in stoechiometric amount; (ii) hydrolysis with a 80–20 vol.% mixture of water + alcohol; (iii) filtration, dispersion in water, addition of lead nitrate (30 mol% excess) and KOH up to [KOH] = 1 M in the final product; (iv) hydrothermal treatment at 265 °C, 45 bar, 2 h; (v) washing and drying.

Depending on the synthesis route, different sintering conditions were chosen. This procedure enables us to produce various fully densified PZT ceramics with and without Ni addition and with different grain sizes. The sintering conditions and some of the characteristics are presented in Table 2.

2.2. X-ray diffraction measurements

High temperature X-ray diffraction measurements were carried out at 550 °C using a Siemens D5000, on powders obtained by crushing sintered samples and annealing at 800 °C for 12 h. In this state, the powders are supposed free of thermal microstrains. Therefore, the broadening effect can be interpreted in terms of crystallite size and specific microstrains linked to chemical fluctuations. XRD measurements at 550 °C were carried out with a step of 0.002° and with a counting time of 10 s. BaF_2 was taken as an internal standard.

2.3. TEM-EDS procedure

After cutting and polishing and dimpling, 30-μm thick samples were Ar ion-milled (Gatan) to electron transparency at 5 kV, with an incident beam angle of 12°. The thin foils were coated with a thin carbon layer to promote electrical charge conduction. Microstructure was investigated with a transmission electron microscope (TEM) Philips CM30, operating with a LaB_6 filament at 300 kV. Quantitative chemical analyses were collected using an X-EDS (X-ray energy dispersive spectroscopy) attachment in the STEM mode (scanning TEM) using beam diameters of about 5 nm. X-rays were detected using a Si detector (Noran) with an ultra-thin window. Relative concentrations were obtained using a Vantage® software (version 2.3.2). K-factors for Zr and Ti were experimentally determined by the parameterless method [6] using oxide standards. Theoretical density of samples were taken at 8.00 g cm^{-3}. The thickness determination of the analyzed area for the absorption correction procedure was based on the principle of electro-neutrality valid for ionic and stoichiometric compounds [7]. When recording the concentration profiles performed across domain boundaries, care was taken to obtain compositions with minimum overlap effects by orienting the interfaces parallel to the electron beam.

3. Results

3.1. X-ray diffraction

Peak broadening for the four powders versus diffraction angle is presented at Fig. 1. It can be seen that the broadening is dependent on diffraction angle meaning that d-spacing fluctuations depend on crystallographic orientation. It is therefore doubtful that from this broadening effect we could extract more information about chemical fluctuations.

Table 2
Sintering conditions and some characteristics of the as obtained ceramics

Sintered materials	Powder synthesis route	Sintering conditions	Relative density[a] (%)	Grain size[b] (μm)	Q_m[c]
C	Oxide	1150 °C 2 h	96.6	3.3 ± 0.5	90 ± 10
C–Ni	Oxide	1150 °C 2 h	92.2	7.9 ± 0.7	1207 ± 134
H	Hydrothermal	950 °C 4 h	95.0	4.1 ± 0.1	2472 ± 115
H–Ni	Hydrothermal	950 °C 4 h	95.5	6.5 ± 0.7	1579 ± 112

[a] Theoretical value is taken at 8.00 g cm^{-3}.
[b] By SEM observations on etched ceramics: of intercepted line method on 80–150 grains.
[c] Mechanical quality factor.

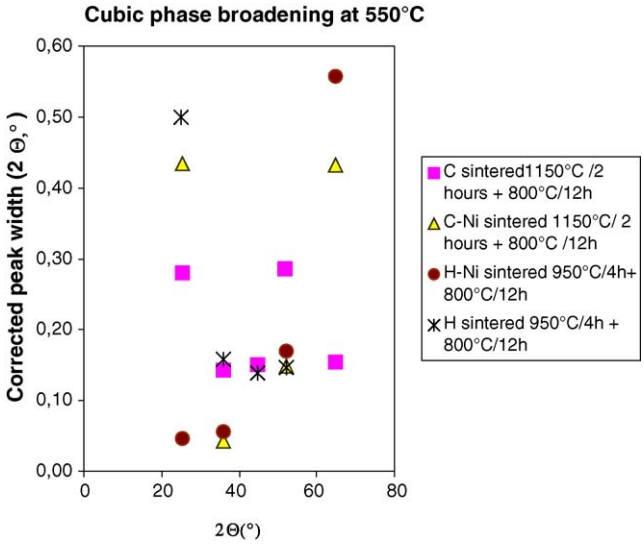

Fig. 1. Corrected peak width of the four powders vs. diffraction angle.

3.2. TEM and EDS analysis

3.2.1. Incorporation of dopants

Local analyses were carried out on the four ceramics. All the ceramics appear to be homogeneously doped. For each one, several local analyses were carried out on a grain, some at boundaries and by comparing several grains. No significant segregation of dopants is observed. Whatever the ceramic analyzed, they appear to be homogeneously doped. Some precipitates are observed in sample C–Ni. Local analysis confirmed them as almost pure zirconia. As an example, we show on Figs. 2 and 3 TEM observation of ceramics H–Ni and C–Ni. For each one, the grain boundary appears to be almost pure. Ferroelectric domains are observed inside grains. Specific precipitation of zirconia is pointed out in ceramic C–Ni.

3.2.2. Chemical composition homogeneity

During the same experiments, Zr and Ti concentrations were measured. Results are presented in Table 3. Different sets of analysis were carried out. We have chosen specific grains (small ones, big ones, in order to be representative for the whole microstructure). In each of these grains, several analyses were made. Conversely, we also have made one analysis by grain but in several ones chosen stochastically.

These values have been analyzed from a statistical point of view (variance analysis).

From this analysis, it is shown that, for a specific ceramic, whatever the localization of the set of analysis (in a specific grain, in another, randomly, across a grain), the mean values of Zr/Zr + Ti ratio are comparable with a confidence interval higher than 95%. Testing the accuracy of a set of measurements, it is shown that they are comparable with a confidence interval higher than 95%.

Bulk chemical compositions are in agreement with the X-ray fluorescence analyses ($x = 0.50$ for C and H, $x = 0.49$ for C–Ni, $x = 0.48$ for H–Ni). These values are in the same order of magnitude, but show same trend: for C and H samples the Zr/Ti composition is weakly larger than for the C–Ni and H–Ni samples.

Fig. 2. STEM observation of ceramic H–Ni.

On the other hand, for each sample, the chemical fluctuations amplitude do not significantly differ whether measured from one grain to another, from random analyses or through a grain.

So, it can be concluded than no significant difference exists in a ceramic, concerning the mean values of Zr/Zr + Ti ratios and the width of their distribution. If we consider that these distributions are mainly limited by chemical fluctuation of Zr and Ti concentrations, this means that these chemical fluctuations do not depend of the nature of the grain, the localization of the measurements and are comparable to the mean values of the whole ceramic.

As it has been demonstrated that these ceramics consist of matter without substructuration of Zr and Ti, let us compare them in a global manner.

Theses results are listed in Table 3. For each ceramic, the mean values of Zr/Zr + Ti and deviation from the mean

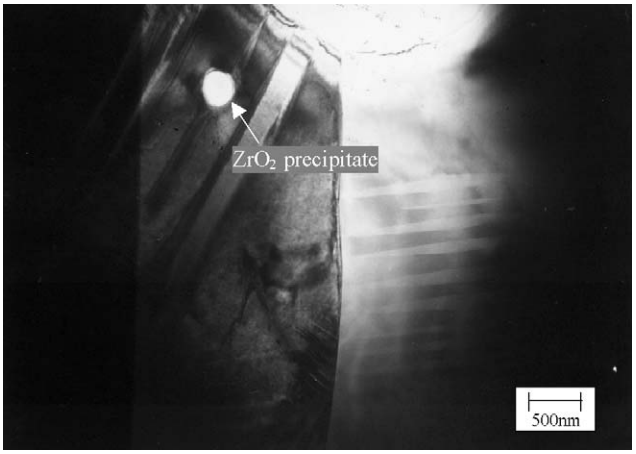

Fig. 3. STEM observation of ceramic C–Ni. Specific precipitation of zirconia is identifed.

Table 3
Results for the four ceramics expressed as mean values of $x = (Zr/Ti + Zr)$ ratio and deviation from the mean of atomic ratio $x = (Zr/Ti + Zr)$

Ceramics	Grain 1	Grain 2	Grain 3	Randomly	Across a grain	Mean value	Pooled estimate of standard deviation
C						0.4810	0.0148
x	0.498	0.465	0.482	0.483			
$\sigma_{(Zr/Zr + Ti)}$	0.013	0.016	0.014	0.015			
X ICP-AES = 0.50 ± 10^{-2}	3 analyses	4 analyses	2 analyses	3 analyses			
C–Ni						0.4780	0.0093
x	0.486	0.478	0.478	0.478	0.475		
$\sigma_{(Zr/Zr + Ti)}$	0.008	0.011	0.008	0.009	0.010		
X ICP-AES = 0.49 ± 10^{-2}	4 analyses	2 analyses	3 analyses	6 analyses	10 analyses		
H						0.4840	0.0104
x	0.481			0.488			
$\sigma_{(Zr/Zr + Ti)}$	0.013			0.004			
X ICP-AES = 0.50 ± 10^{-2}	4 analyses			3 analyses			
H–Ni						0.4750	0.0096
x	0.475	0.477		0.489	0.472		
$\sigma_{(Zr/Zr + Ti)}$	0.016	0.004		0.014	0.008		
X ICP-AES = 0.48 ± 10^{-2}	3 analyses	3 analyses		3 analyses	14 analyses		

(pooled estimate of standard deviation) are calculated. Mean values are comparable with a probability higher than 95%.

Conversely, if we compare the accuracy of these measurements from a global ceramic point of view (expressed here by the pooled estimate of standard deviation), these values differ significantly in some cases. They are comparable for ceramics containing Nickel addition whatever the nature of powder synthesis route. The value of this standard deviation is 0.009. The accuracy of the measurements are significantly different, with a confidence interval higher than 95%, if we compare the ceramic with and without Ni addition, whatever the process chosen for the synthesis of the powders. The value of this standard deviation is 0.012. Note that thermal treatment of sintering has no specific effect of the width of Zr/Zr + Ti distribution. Hydrothermal synthesized powders are sintered at lower temperature. The thermal treatment leads to the same ceramic from a chemical point of view. PZT ceramics are more homogenous with Ni addition and less homogeneous without Ni addition.

3.2.3. Compositional profiles across ferroelectric domains

Compositional profiles across ferroelectric domains have been recorded, for C–Ni and H–Ni ceramics. The domains measured were limited to those tilted in a way such that domain wall planes were parallel to the electron beam direction. Results are given in Fig. 4a and b and Table 4, and in Fig. 5a and b and Table 5, for C–Ni and H–Ni, respectively.

If we analyze these results, it can be concluded that average values of Zr/Ti + Zr ratio of bright and dark areas are identical (>95%). The same conclusion can be taken concerning standard deviation.

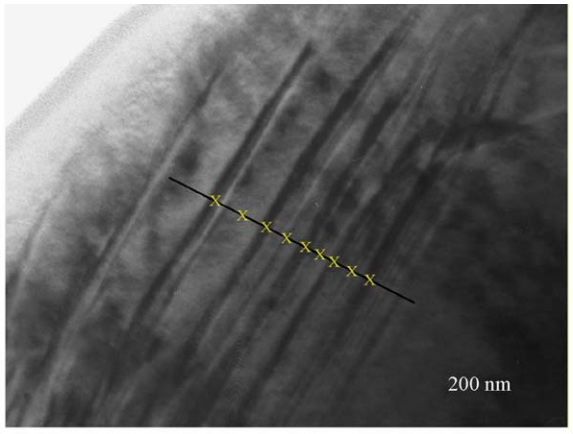

(a)

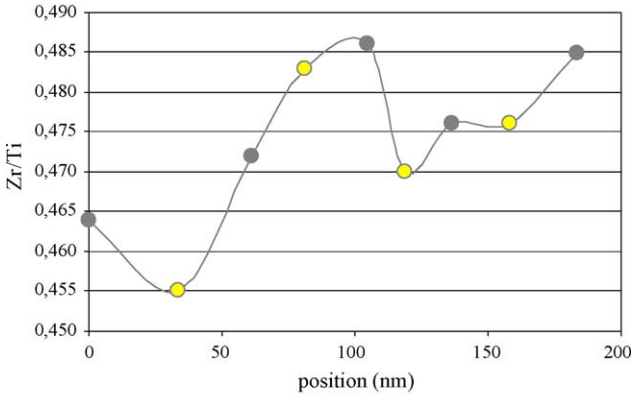

(b)

Fig. 4. Ceramic C–Ni (a) local analyses in a grain across ferroelectric domains; (b) results of analyses (grey points correspond to domains in dark contrast and the other to ones in bright contrast).

Table 4
Experimental values of Zr/Ti + Zr composition ratio determined as localized in Fig. 2a

Mean values of Zr/Ti + Zr (9 analyses)	0.474
Mean values of Zr/Ti + Zr on dark areas (5 analyses)	0.477
Mean values of Zr/Ti + Zr on bright areas (4 anlyses)	0.471
Deviation from the mean (total)	0.010
Deviation from the mean (dark areas)	0.009
Deviation from the mean (bright areas)	0.012

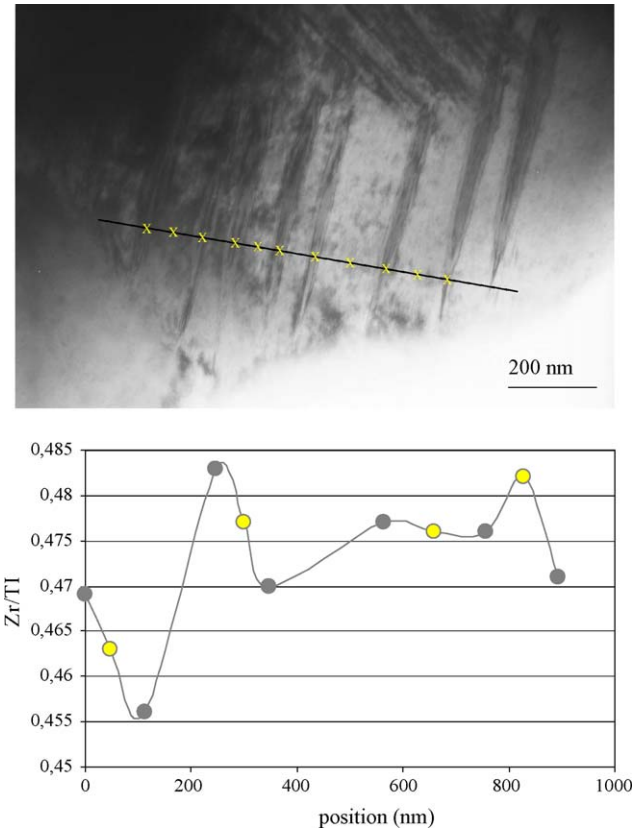

Fig. 5. Ceramic H–Ni (a) local analyses in a grain across ferroelectric domains; (b) results of analyses (grey points correspond to domains in dark contrast and the other to ones in bright contrast).

Therefore, it is obvious that no significant composition gradient or clear composition modulation of Zr/Ti + Zr ratio was detected, for the spatial resolution achieved in the present analytical STEM examination, by comparing the value of one ferroelectric domain to an adjacent one.

Table 5
Experimental values of Zr/Ti + Zr composition ratio determined as localized in Fig. 3a

Mean values of Zr/Ti + Zr (11 analyses)	0.473
Mean values of Zr/Ti + Zr on dark areas (7 analyses)	0.472
Mean values of Zr/Ti + Zr on bright areas (4 analyses)	0.475
Deviation from the mean (total)	0.008
Deviation from the mean (dark areas)	0.008
Deviation from the mean (bright areas)	0.008

If we compare the two ceramics with their global composition, pooled estimate of standard deviations (i.e. indicative chemical fluctuations) for C–Ni and H–Ni samples, are comparable. It is confirmed that there is no significant partitioning of Zr and Ti in the ceramics. As they both contain Ni addition, standard group deviation of Zr/Zr + Ti is comparable.

4. Discussion and conclusion

Ni addition effect can be estimated by comparing both hydrothermal and solid state synthesized powders. Ni acts as a sintering aid and promotes grain growth during sintering. We have shown [5] that for solid-state synthesized powders, Ni addition favors densification and decreases the sintering temperature range by 100 °C. For hydrothermal powders, Ni addition does not affect significantly the sintering temperature range. The powders are intrinsically reactive wherever they are doped with Ni or not. For solid-state synthesized powder, the mean grain size is increased by 2.3 (3.3–7.9 μm) if Ni is added. As Ni is less effective for hydrothermal powders, but also as the sintering conditions (950 °C/2 h) for these more reactive powders are lower, the mean grain size is only increased by 1.6 (4.1–6.5 μm). These conditions are likely to promote densification prior to grain growth. If we analyze Ni addition effect with respect to the quality factor Q, Ni addition has a strong and positive effect on ceramic C and a slight and negative one on ceramic H. It seems that Ni addition has a dual and contradictory effect. On the one hand, it favors densification and promotes grain growth. This effect is very positive to mechanical factor and is predominant in presence of a less reactive powder, i.e. a solid state synthesized one. On the other hand, Ni addition seems intrinsically detrimental to the mechanical factor, but at a lower level. This second effect is overtaken by the sintering aid effect with solid-state synthesized powders. For hydrothermal powder, as there is a negligible sintering aid effect, presence of Ni acts is a detrimental. If trying to link Q values with estimated chemical fluctuation (pooled estimate of standard deviation of Zr/Ti + Zr ratios), it appears that there is no. Ni addition is beneficial on Q values for solid-state synthesized powders, and is detrimental for hydrothermal ones. On the contrary, Ni addition is beneficial on chemical fluctuation on both the two routes.

At this state of work, Q value seems not to be related to a low value of Zr/Zr + Ti fluctuation; in our case, the experimental area corresponds to relatively low values of chemical fluctuation. The best Q values should be obtained starting from very reactive powders without nickel addition. At the same time, this ceramic does not exhibit the lower value of Zr/Zr + Ti fluctuation ratio.

It seems that the lowest compositional fluctuations ≈0.009 obtained for our ceramics are an upper limit. It is not evident that homogeneity can be enhanced by sintering at upper temperature and/or for longer dwell time as it is

demonstrated by the non-effect of Ni addition (and grain growth) for hydrothermal powders. Noheda et al. [2] have estimated chemical fluctuation by means of high temperature X-ray diffraction. Their value raises ±0.003, which is lower than our observation. Let us remark that both results are in the same order of magnitude, demonstrating the accuracy of the estimation of internal chemical fluctuation starting form the broadening of diffraction peaks. The differences between these two values can be related either with the imperfect state of sintering of our ceramics and with their doping or either with the statistical approach of our results. On another hand, our powder diffraction peak broadening is not independent of crystallographic orientation, preventing us to perform any estimation of chemical fluctuation. This shows that results reported in the literature of have to be analysed very carefully, and a very fine approach is necessary as this of Noheda et al. [2].

Our main results consist in the impossibility to observe some significant internal composition fluctuations between ferroelectric domains neither between grains. The local analyses were chosen hazardously whatever the size of the grain. At the level of the used spatial resolution, grains appear as monophasic as the entire ceramic. The magnitude of the grain boundary motion is not, in our case, the cause of flattening of internal fluctuations. The dependence of internal fluctuation with grain growth $\Delta x \approx G^{-3/2}$ observed by Soares et al. [4] has been observed for higher values of internal fluctuations than in our case. We can conclude that flattening of internal fluctuations occurs by means of grain boundary motion as long as internal fluctuation remains at a high level (more than 0.012). The model proposed by Cao and modified by Soares [3,4] is valid. Below, flattening occurs by volume diffusion and is independent of grain growth.

References

[1] B. Jaffe, W.R. Cook, H. Jaffe, Piezoelectric Ceramics, Academic Press, London, 1971.
[2] B. Noheda, J.A. Gonzalo, L.E. Cross, R. Guo, S.E. Park, D.E. Cox, G. Shirane, A tetragonal-to-monoclinic phase transition in a ferroelectric perovskite: the structure of $PbZr_{0.52}Ti_{0.48}O_3$, Phys. Rev. B 61 (2000) 8687.
[3] W. Cao, L.E. Cross, Theoretical model for the morphotropic phase boundary in lead zirconate–lead titanate solid solution, Phys. Rev. B 47 (9) (1993) 4825–4830.
[4] M.R. Soares, A.M.R. Senos, P.Q. Mantas, Phase coexistence in PZT ceramics, J. Eur. Ceram. Soc. 19 (1999) 1865–1871.
[5] N. Texier-Mandoki, C. Courtois, P. Champagne, A. Leriche, Hydrothermal synthesis of doped PZT powders: sintering and ceramic properties, Mater. Lett. 58 (2004) 2489–2493.
[6] E. Van Cappellen, The parameterless correction method in X-ray microanalysis, Microsc. Microanal. Microstruct. 1 (1990) 1–22.
[7] E. Van Cappellen, J.C. Doukhan, Quantitative transmission X-ray microanalysis of ionic compounds, Ultramicroscopy 53 (1994) 343-L349.